

Effusivity Sensor Package (ESP) System for Process Monitoring and Control

M. Emanuel

Abstract

The effusivity sensor package (ESP) system measures effusivity of materials, based on the transient plane source method. It is used mainly as an on-line or in-line process monitoring and control system in various industries such as pharmaceutical and cosmetics. Examples of applications are real time monitoring of the uniformity of blended powders in motion, and monitoring of drying processes.

The system combines a reduced calibration technique with improved algorithms that compensate for variations in sensor temperature, thus enabling reliable effusivity measurements seamlessly in a wide range of temperatures (20°C to 70°C).

The review includes theoretical principles, design considerations for the sensor and system, sensor calibration and uncertainty evaluation of measurements. Finally typical experimental results are reported.

Introduction

Effusivity is defined as the square root of the product of thermal conductivity, λ , density, ρ and specific heat capacity, c_p , ($\sqrt{\lambda \cdot \rho \cdot c_p}$) and has units of $\frac{W\sqrt{s}}{m^2 K}$. The ESP system measures effusivity directly.

The system comprises an effusivity sensor, control electronics and computer software. The sensor operation is based on the transient plane source method. It has a central heater/sensor element in the shape of a spiral surrounded by a guard ring. The guard ring generates heat in addition to the spiral heater, thus, approximating a one-dimensional heat flow from the sensor into the material under test in contact with the sensor. The voltage drop on the spiral heater is measured before and during the transient. The voltage data is then translated into the effusivity value of the tested material.

If the system is calibrated for thermal conductivity, the conductivity may be calculated from the voltage data by Mathis' patented iterative method [1,2,3] or by alternative methods [4].

Theory

The heat equation in one dimension with a constant supply of heat per time per volume, G' , is given below:

$$\rho c_p \frac{\partial T}{\partial t} = \lambda \frac{\partial^2 T}{\partial x^2} + G' \quad (1)$$

Assume two semi-infinite media in contact with heat generated at the interface at a constant rate per unit area per unit time. Further assume that one medium is represented by the effusivity sensor, and the other medium is the material under test. Both media are at the same temperature after contact between them has been established. The solution of equation (1) follows these expressions [5]:

$$\Delta T_1(x, t) = \frac{2G\sqrt{t}}{e_1 + e_2} \operatorname{ierfc} \frac{|x|}{2\sqrt{a_1 \cdot t}} \quad \text{for } x < 0, t > 0 \quad (2)$$

$$\Delta T_2(x, t) = \frac{2G\sqrt{t}}{e_1 + e_2} \operatorname{ierfc} \frac{x}{2\sqrt{a_2 \cdot t}} \quad \text{for } x \geq 0, t > 0 \quad (3)$$

Where $\Delta T(x, t)$ is the change in medium temperature (K), G is the power flux supplied to the sensor (W/m^2), t is the time measured from start of the process (s), e_1, e_2 indicate the equivalent effusivity of the sensor ($\sqrt{\lambda_1 \cdot c_{p1} \cdot \rho_1}$), and the material under test ($\sqrt{\lambda_2 \cdot c_{p2} \cdot \rho_2}$) and a_1, a_2 denote the equivalent diffusivity of the sensor and the sample, respectively.

If no thermal contact resistance exists at the interface, $T_1(x = 0, t) = T_2(x = 0, t)$ at all points with $x = 0$. For $x = 0$ equations (2) and (3) are reduced to:

$$\Delta T(x = 0, t) = \frac{1.1284G\sqrt{t}}{e_1 + e_2} \quad (4)$$

Equation (4) is accurate only for the case of two semi-infinite media creating a perfect one-dimensional heat flow. To find a good approximation for the case of a finite sensor, it is necessary to create an approximate one-dimensional heat flow at the sensor surface. This condition can be satisfied by using a guard ring around the heater, and optimizing the resistances of the heater/sensor and guard, and the current supplied to them.

The control electronics supply accurate current to the heater and guard, and measure the heater's voltage before and during the transient process. The signal is therefore a voltage signal and has to be translated to temperature. This is done by considering the temperature coefficient of resistivity (TCR) of the sensor.

Assuming perfect linearity of the sensor TCR, the relationship between the sensor resistance and its temperature is given by:

$$R(T) = R_0(1 + \alpha T) = R_0 + \alpha R_0 T \quad (5)$$

Where $R(T)$ is the resistance of the sensor at temperature T , R_0 is the sensor resistance at 0°C , T is the sensor temperature ($^\circ\text{C}$), α is the TCR and A is the slope.

The change in the sensor resistance during the transient is

$$\Delta R(t) = R(t) - R(t=0) = A\Delta T(x=0, t) \quad (6)$$

And the voltage change on the sensor is, assuming the current is constant throughout the transient,

$$\Delta V(t) = I\Delta R(t) = IA\Delta T(x=0, t) \quad (7)$$

Equation (4) can be written as:

$$\Delta T(x=0, t) = \frac{1.1284G\sqrt{t}}{e_1 + e_2} \quad (8)$$

Therefore

$$\Delta V(t) = \frac{1.1284IAG\sqrt{t}}{e_1 + e_2} \quad (9)$$

Equation (9) can also be written as:

$$\Delta V(t) = m\sqrt{t} \quad (10)$$

Where m is the slope,

$$m = \frac{1.1284IAG}{e_1 + e_2} \quad (11)$$

$$\frac{1}{m} = \frac{e_1 + e_2}{1.1284IAG} \quad (12)$$

If e_2 is 0, i.e. the sensor response is measured in vacuum, then:

$$\frac{1}{m_v} = \frac{e_1}{1.1284IAG} \quad (13)$$

The value of (e_1/IAG) is a sensor/system figure of merit, and depends only on sensor characteristics and supplied power, and can be used for calibration of sensor response versus effusivity of material under test. Since no material is involved in this calibration point, the measured slope in vacuum is very accurate and an excellent reference point. Rearranging equation (12), it can be written as:

$$\frac{1}{m} = M \cdot e_2 + C \quad (14)$$

Where M is the slope of the effusivity calibration line and C is the intercept. M is given by:

$$M = \frac{1}{1.1284IAG} \quad (15)$$

And C is:

$$C = \frac{e_1}{1.1284IAG} \quad (16)$$

M can be calculated from the system parameters, or experimentally determined by measuring two or more materials with known effusivities. C is the $1/m$ value for vacuum and must be measured, since the sensor equivalent effusivity may be slightly different from one sensor to another. Once C is measured and M is calculated, the equivalent effusivity of the sensor is readily evaluated from:

$$e_1 = \frac{C}{M} \quad (17)$$

To calculate the effusivity of the material under test from (14) one can use:

$$e_2 = \frac{\frac{1}{m} - C}{M} \quad (18)$$

Where $1/m$ is the inverse of the voltage versus \sqrt{t} slope measured for this material, and M and C are the slope and intercept of the effusivity calibration curve for a given sensor, respectively.

Temperature considerations in effusivity measurements

As seen above, two parameters, M and C are required for effusivity calibration at a given set of conditions. In real applications the environment temperature may change and affect the system measurement accuracy. Hence, a compensation mechanism is required to ensure accurate measurements under varying conditions.

Equation (15) suggests that M will remain constant in temperature as long as the denominator is constant. Since

$$G = \frac{I^2 R}{S} \quad (19)$$

Where S is the sensor area, it turns out that

$$M = \frac{S}{1.1284A(I^3 R)} \quad (20)$$

The sensor area, S , and A are constant in the temperature range of interest (20°C to 70°C). Therefore, if the product $(I^3 R)$ is kept constant, M will remain constant. The system employs an automatic power correction algorithm, which keeps $(I^3 R)$ constant at any ambient temperature. This is executed prior to a test. The power correction also preserves the approximate one-dimensional heat flow condition.

The same applies also to the intercept C , since C has the same denominator in equation (16). The sensor equivalent effusivity, e_l , changes with temperature since it depends on the sensor materials and construction. Experiments show that e_l is approximately linear with temperature in the range it was measured, 20°C to 70°C. It changes approximately 0.25% per degree Celsius.

Uncertainty analysis

General

Variations in effusivity measurements have three significant sources: errors from equipment, quality of thermal contact between the sensor and the material under test, and variations in the material (e.g. dry powder versus same powder with some moisture content). The first two factors are related to the equipment and method of measurement, and, in general, must be carefully considered. The third source of variation comes from a real variation in the material under test.

Material

Variations in material under test will change the heat transfer characteristics. A good example is humidity content in powders. Water has a higher effusivity than many powders, and therefore a change in humidity content will change the measured effusivity. This source of variation is not treated here as a measurement error, but rather as the measured characteristic.

Another source of material variation (specifically related to powders) is compaction. The effusivity of a powder depends on the amount of air between the particles. When compaction occurs, the measured effusivity is higher. Therefore, to have repeatable results on powders, a good material handling method must be followed.

Thermal Contact

The quality of contact between the sensor surface and the material is critical for accurate and repeatable measurements. Powders, liquids and creams usually create a good contact with the sensor, but it is not always the case with solids. For liquids, creams and powders, contact resistance can be regarded as negligible as long as the particle size is much smaller than the sensor.

Equipment

Equipment errors may originate from variations in the current source due to changes in environment temperature, short term and long term drifts, change in sensor resistance (and hence supplied power) during the transient measurement and change in sensor resistance (and hence supplied power) due to initial sensor temperature. Additional errors may come from the voltage measurement circuitry.

From equation (18) the relative variance in e_2 can be calculated by:

$$\left[\frac{U(e_2)}{e_2} \right]^2 = \left[\frac{U(m)}{m} \right]^2 + \left[\frac{U(C)}{C} \right]^2 + \left[\frac{U(M)}{M} \right]^2 \quad (21)$$

Since C and M are constant during the transient measurements, the only contributor to variance is m. It can be shown that

$$\left[\frac{U(m)}{m} \right]^2 = \left[\frac{3U(I)}{I} \right]^2 + \left[\frac{U(R)}{R} \right]^2 \quad (22)$$

And therefore:

$$\left[\frac{U(e_2)}{e_2} \right]^2 = \left[\frac{3U(I)}{I} \right]^2 + \left[\frac{U(R)}{R} \right]^2 \quad (23)$$

The variation in e_2 is affected by the variations in current source and sensor resistance during the transient, and variations between different measurements.

To evaluate the error from the change in sensor resistance during a transient, assume a 1 to 1.5 K change in sensor temperature (~0.5-1.5 s transient) for the range of materials used with the system. The platinum wire of the sensor has a TCR of 0.0037 K⁻¹. During the transient, the sensor resistance changes 0.37-0.56%, and the power supplied to the sensor changes by the same amount. However, since the calibration of the sensor is performed in exactly the same manner as the measurement of the material under test, this error is calibrated out for most practical cases, leaving a very small residual error of less than 0.1%.

As mentioned earlier, the power supplied to the sensor is automatically corrected at the beginning of each sampling, to the extent of the precision of the current source. The error coming from the current source depends on how well it is designed and compensated for short term and long term drifts.

As an example, with measured errors less than 0.1% in the current source and less than 0.06% in the voltage measurement circuitry, effusivity measurements can be made with overall RSD (relative standard deviation) of less than 0.5%.

Sensor design

The sensor is designed to satisfy certain requirements for the intended applications. The main ones are: direct measurement of effusivity, on-line measurements in rotational moving vessels, manufactureable, rigid, compact, completely sealed and high sensitivity.

The first requirement implies that the sensor should create one-dimensional heat flow to the material under test. This was achieved by using a guard heater around the main heater and sensing element.

The second requirement means that the sampling time must be short to accommodate fast rotating vessels, such as blenders. The third and fourth requirements were achieved by using a known thick film technology. The sensing

element is platinum, deposited on a thin alumina substrate. High sensitivity was obtained by increasing the resistance of the sensing element to about $27\ \Omega$. This is easily achievable using the thick film technology.

Figure 1 shows a simulation of the sensor temperature and heat flow at two seconds after heat is supplied. A cross section of half of the sensor is shown. The sensor surface is at 0 mm, the back of the sensor is to the left and on the right is the material under test (effusivity of $500\ \text{W}\sqrt{\text{s}}/\text{m}^2\text{K}$). From the isothermal lines parallel to the sensor surface one can see that the heat wave propagates almost in one dimension only in the area of the sensor elements, represented by 10 rectangles. The guard ring (narrow rectangle at top) protects the sensor element from losing a significant amount of heat to the edges. This supports the assumption that led to equations (2) and (3).

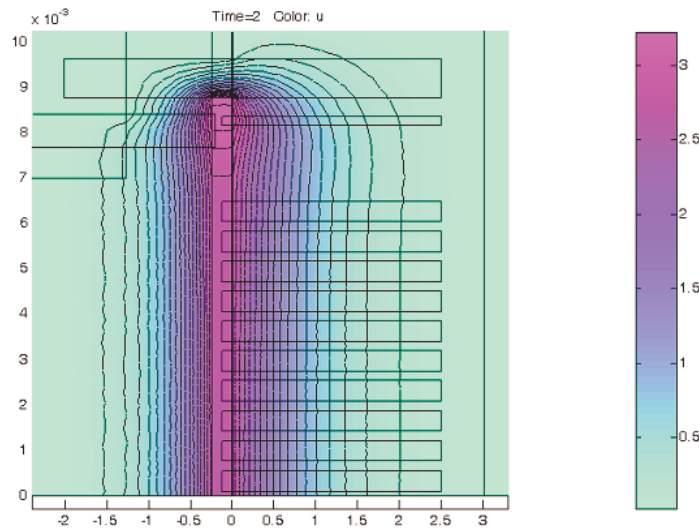


Figure 1. FEM simulation of sensor/material temperature after 2 seconds of heating. X-axis is in mm and Y-axis is in m.

Figure 2 shows the sensor temperature change versus square root of time for 0 to 2 s, with and without sensor substrate for comparison. The linear region is used for calibration of the sensor and measurement of the effusivity of the material under test.

In the case of no substrate (e_1 very small relative to e_2) the slope is steep. In the other case (e_1 comparable to e_2) the slope is smaller as predicted in equation (8). Additionally, it takes longer to achieve linearity because of the substrate's heat capacity.

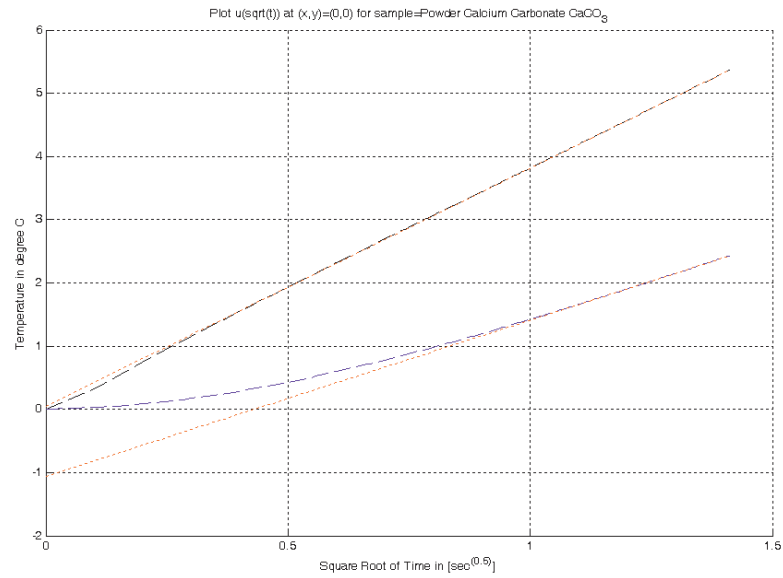


Figure 2. Simulation of sensor surface temperature during the transient

Figure 3 shows the sensor packaged in its stainless steel housing. The sensitive element is the spiral. The guard ring can be seen near the edge of the alumina (green area). The red circle is glue and beyond that is the stainless steel housing.

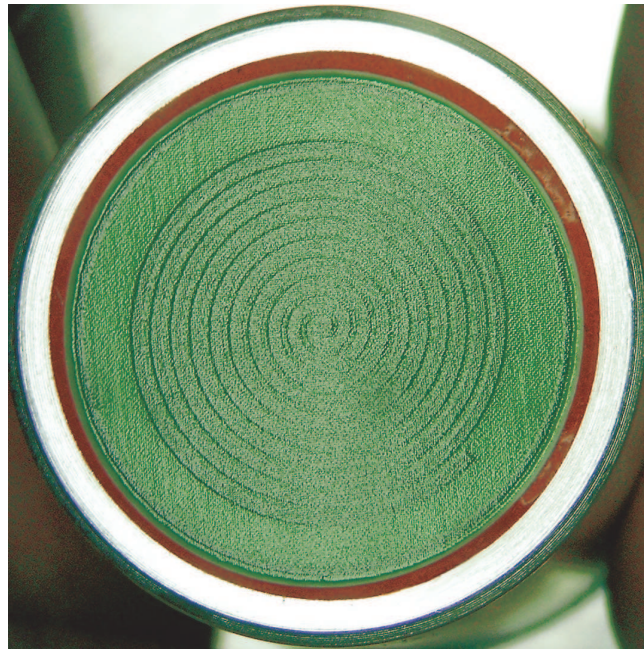


Figure 3. Surface of effusivity sensor, packaged in a stainless steel housing

Electronics

A simplified circuit diagram of the sensor electronics is depicted in Figure 4. A microprocessor controls the circuit. The sensor is supplied with current from a programmable current source. The sensor voltage is fed into a differential amplifier G1 using a 4-wire technique. The initial amplifier output is converted to a digital value by an ADC and stored by the microprocessor. It is then used as reference in the differential amplifier G2. The output from G2 is the net sensor signal.

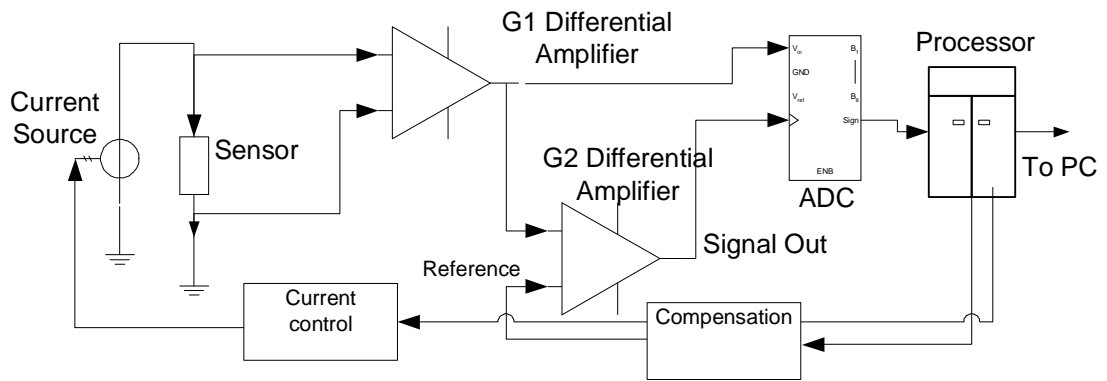


Figure 4. Simplified sensor electronics block diagram

Experimental: sensor calibrations

The effusivity sensor undergoes two calibrations. One is the calibration of the sensor resistance versus temperature (TCR calibration) and the other is the effusivity calibration.

TCR calibration

An example of TCR calibration of three sensors is depicted in Figure 5. The data shows good linearity over a wide temperature range, in support of equation (5).

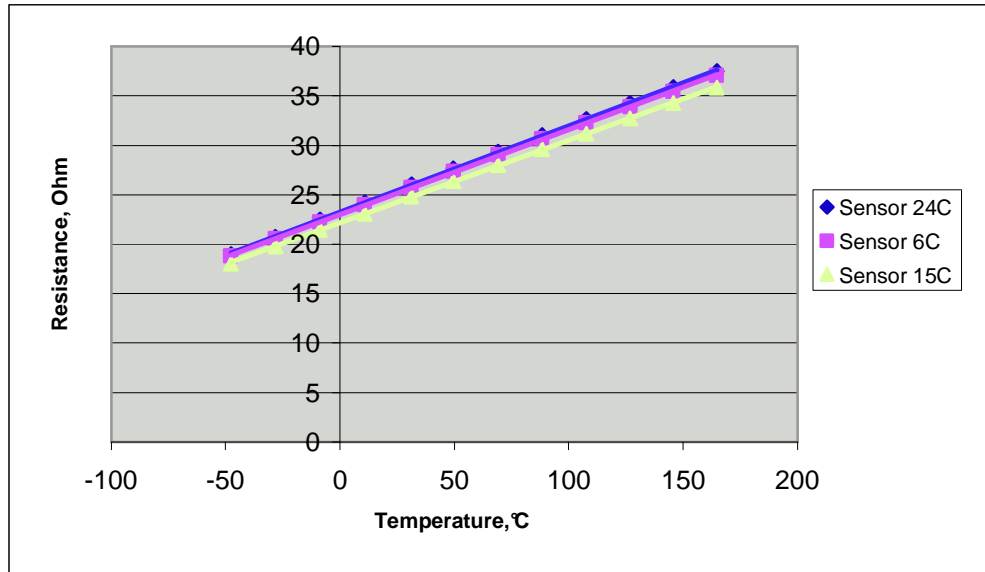


Figure 5. TCR calibration of sensors

Basic effusivity calibration

Figure 6 is a typical voltage- \sqrt{t} measurement, obtained with the system on PDMS (Polydimethyl Siloxane supplied by DOW Corning®), effusivity 493 $\text{W}\sqrt{\text{s}}/\text{m}^2\text{K}$. The slope is calculated in the region confined by the vertical lines (0.7 $\sqrt{\text{s}}$ and 1.22 $\sqrt{\text{s}}$).

An example of an effusivity calibration is given in Figure 7, for an effusivity range of 0-1650 $\text{W}\sqrt{\text{s}}/\text{m}^2\text{K}$. The calibration line was obtained by measuring the $1/m$ sensor response in vacuum and with two materials with known effusivities under stabilized conditions (PDMS 493 and water gel 1641 $\text{W}\sqrt{\text{s}}/\text{m}^2\text{K}$). The line is linear, confirming the validity of equation (14) and the assumptions that led to it.

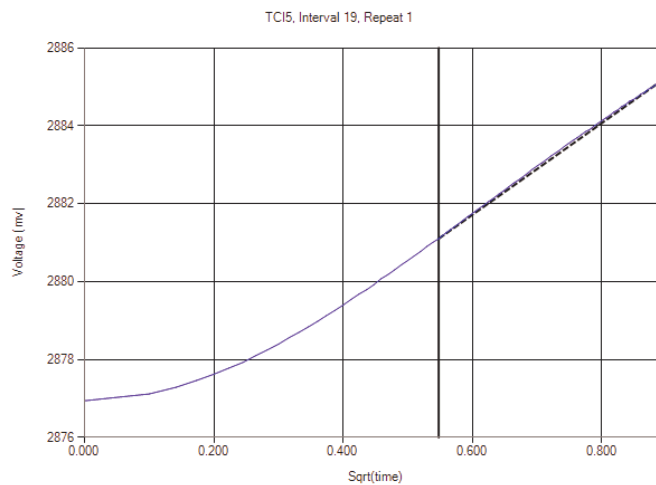


Figure 6. Typical voltage versus square root of time transient

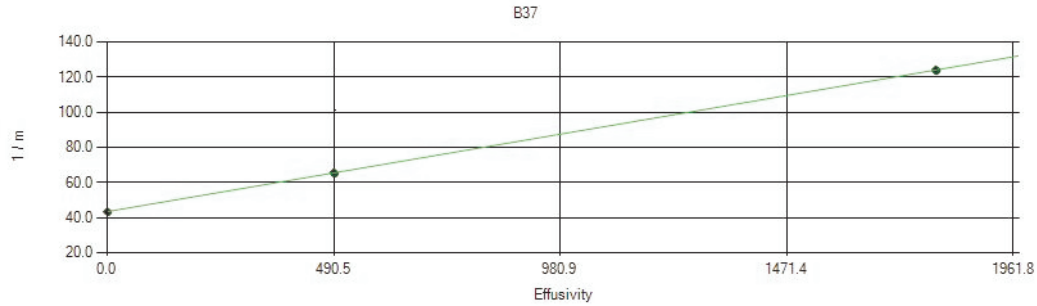


Figure 7. Effusivity calibration with vacuum, PDMS and water gel

Effusivity calibration at various temperatures

Sensors were calibrated for effusivity at 20°C and 70°C, in vacuum and with PDMS. No power correction was applied. The slope M and intercept C of some sensors are listed in Table I. The slope M changed significantly between the two temperatures, because of the sensor resistance, affecting the power in equation (15). C also changed a few percentage points.

Table I. Effusivity calibration without power correction. M is in ($\text{m}^2\text{K}/\text{WV}$) and C is in ($\sqrt{\text{s}/\text{V}}$)

Sensor	21.4°C		70.0°C		Delta M		Delta C	
	M	C	M	C	Change	% Change	Change	% Change
B45	0.05045	38.6526	0.03914	39.8761	-0.0113	-22.4%	1.22	3.2%
B49	0.05437	44.1644	0.04808	44.8666	-0.0063	-11.6%	0.70	1.6%
B69	0.05014	43.4656	N/A	N/A	-	-	-	-

Table II. Effusivity calibration with power correction. M is in ($\text{m}^2\text{K}/\text{WV}$) and C is in ($\sqrt{\text{s}/\text{V}}$)

Sensor	20.1°C		69.0°C		Delta M		Delta C	
	M	C	M	C	Change	% Change	Change	% Change
B45	0.04897	40.213	0.04917	45.412	0.00020	0.41%	5.199	12.9%
B49	0.05402	42.260	0.05422	48.016	0.00020	0.37%	5.756	13.6%
B69	0.05012	43.149	0.05041	48.495	0.00029	0.58%	5.346	12.4%

Table II shows results of same sensors after re-calibration, this time with automatic power correction. It can be seen that the power correction algorithm indeed corrects the slope M of the effusivity calibration to better than 1%. This verifies equation (20) and the discussion that followed. This also means that the effusivity calibration can be reduced to one point only, i.e. vacuum. M can be calculated from equation (20), and it should be good for any testing temperature.

One can also see in Table II that the variation in C is larger than in Table I. As mentioned before, C varies because the sensor's equivalent effusivity grows with

temperature. If no power correction is applied, the denominator of C , equation (16), also becomes larger, thus somewhat compensating for the sensor effusivity. Table II therefore shows the net increase in sensor equivalent effusivity. The change in C is translated approximately to sensor effusivity increase of $\sim 100 \text{ W}\sqrt{\text{s/m}^2\text{K}}$ between 20°C to 70°C .

C as a function of temperature is given in Figure 8. It is almost linear in the temperature range of interest, and therefore can be approximated to a straight line. Alternatively, it may be regressed to a polynomial fit.

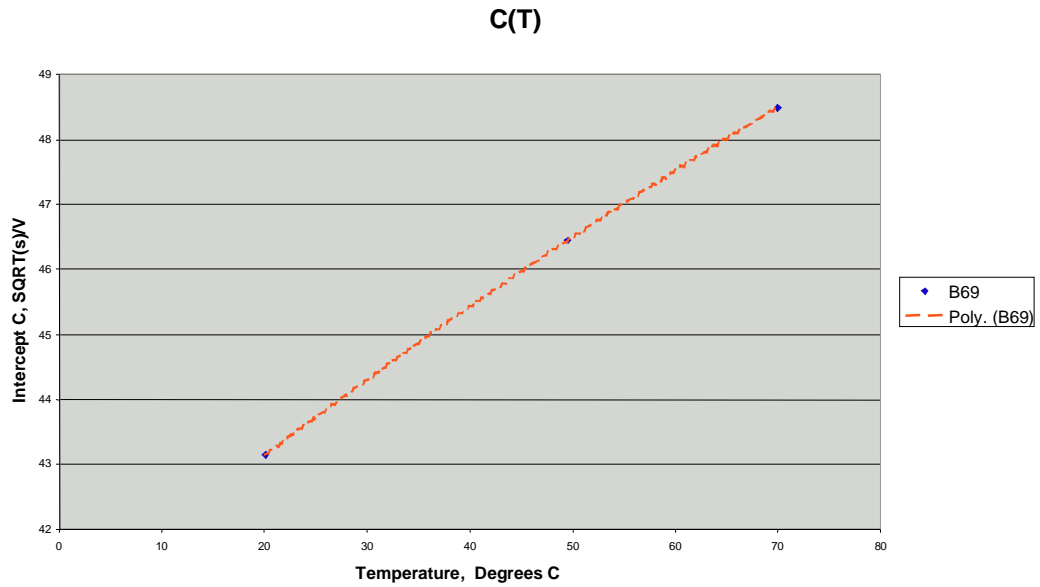


Figure 8. Typical intercept C as function of temperature

Experimental: Testing materials

In regular testing the system measures the sensor temperature prior to the test, adjusts the power as required, calculates the applicable C and finally calculates the material effusivity. Sensor B69 was used to measure PDMS. The system used the parameter M shown in Table II and a $C(T)$ line for this sensor, Figure 8. The sensor was stabilized at 50°C and then obtained 20 samples. The average value was $489.5 \text{ W}\sqrt{\text{s/m}^2\text{K}}$ with RSD of 0.3%. The value of PDMS at 50°C is $491.5 \text{ W}\sqrt{\text{s/m}^2\text{K}}$. That is 0.4% deviation from the ideal value.

Conclusions

The effusivity sensor was designed for a one-dimensional heat flow. Simulations and test results confirm that the sensor indeed creates a nearly one-dimensional heat flow for a wide range of tested materials.

It is shown that a combination of analytical solution, power correction and sensor calibration provides a continuous operation in a wide temperature range with a good accuracy.

Future work will concentrate on adaptation of the effusivity sensor and system for measuring thermal conductivity of liquids, solids and thin films.

Acknowledgements

The author thanks his colleagues at Mathis Instruments for the design and execution of the project, and Dr. Jules Picot, UNB, Fredericton, Canada for helping with the selection and measuring of calibration materials. The work was supported by the Atlantic Innovation Fund (AIF).

References

1. Mathis, N. and C. Chandler 2004. *Direct Thermal Conductivity Measurement Technique*, United States Patent, US 6,676,281 B1.
2. Chandler, C., B. Canney and N. Mathis, 2003. "Validation of the Algorithm for Direct Thermal Conductivity Measurement with Modified Hot Wire on Film, Insulation and Liquid," Proceedings of the Twenty-Sixth International Thermal Conductivity Conference.
3. Mathis, N.E., 1999. "New Transient Non-Destructive Technique Measures Thermal Effusivity and Diffusivity", Proceedings of the Twenty-Fifth International Thermal Conductivity Conference.
4. Gustafsson, S.E. 1991. "Transient plane source technique for thermal conductivity and thermal diffusivity measurements of solid materials," *Rev. Sci. Instrum.* 62:797-804.
5. Carslaw, H.S. and J.C. Jaeger, 1959. *Heat Conduction in Solids*. Chapter II. Oxford: Oxford University Press.
6. See for example, Guide To The Expression Of Uncertainty In Measurement. ISO, Geneva, Switzerland 1993. (ISBN 92-67-10188-9).